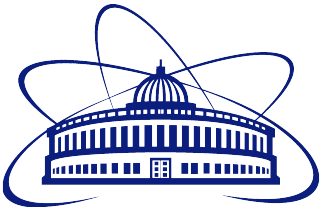

JOINT INSTITUTE FOR NUCLEAR RESEARCH
Veksler and Baldin laboratory of High Energy Physics

FINAL REPORT ON THE START PROGRAMME

Estimation of corona polarization for Λ hyperons

Supervisor:
Dra. Ivonne Alicia Maldonado Cervantes

Student:
José Jorge Medina Serna, Mexico
Nuclear Sciences Institute,
National Autonomous University of Mexico

Participation period:
July 3rd – August 25th,
Summer session, 2023

Dubna, 2023

Abstract

An estimation of polarization of Λ hyperon using the projection and flow method for jetty-like and isotropic events was carried on for Monte Carlo and reconstructed data using the official Monte Carlo data sets of MPD collaboration. The identification of jetty and isotropic events was made trough the transverse sphericity event shape variable. Such separation of events is related with the elliptic flow and the corona contribution to polarization in the Core-Corona model. Such analysis required the implementation of the Analysis Framework in MPDroot. Results show a small difference between jetty and isotropic events, but isotropic events seems to be a little larger. It was performed a reconstruction of Λ in order to compare the obtained Monte Carlo results with reconstructed data. Polarization for reconstructed data behaves similar to Monte Carlo, but is necessary to improve the reconstruction and clean the signal, this is still a work in progress.

Acknowledges

This project is prepared in fulfilment of the requirement for the START program at JINR. I owe my deepest gratitude to the STAR group at Veskler and Baldin Laboratory of High Energy Physics, Joint Institute of Nuclear Research for providing me with an opportunity through the START program to work on this project.

I also extend my gratitude towards my project supervisor and mentor, Dr Ivonne Alicia Maldonado Cervantes whose guidance and expertise have been invaluable in steering me towards success.

Finally, I would like to thank my friends Santiago Bernal Langarica, Rodrigo Garcia Formenti Mendieta, Rodrigo Guzman Castro and Nishant Gaurav for their constant encouragement throughout the START program. I acknowledge the contributions of everyone who supported me in the creation of this project report.

Contents

1 Introduction **4**
1.1 Nuclear matter 4
1.2 Nucleotron-based Ion fAcility complex (NICA) 5
1.3 Multi-Purpose Detector (MPD) 6

2 Theoretical framework **8**
2.1 Core Corona approach 8
2.2 Estimation of the polarization from the corona 9
2.3 Event shape variables 10

3 Methodology **12**
3.1 General methodology 12
3.2 MPDroot framework and analysis trains 13
3.2.1 Core-Corona analysis train 13
3.3 Isotropic and jetty events 14
3.4 Reconstruction of Λ 15

4 Results **17**
4.1 Polarization of Monte Carlo data 17
4.2 Invariant mass for reconstructed Λ 25
4.3 Polarization of reconstructed and associated data 25

5 Conclusions **30**

Chapter 1

Introduction

1.1 Nuclear matter

The purpose of this project is to carry out frontier research in one of the most challenging tasks of modern physics; the study of strongly interacting baryonic matter and contribute to a deeper understanding of the properties of nuclear matter in the maximum variance density region of the quantum chromodynamic (QCD) phase diagram, which gives us information about the evolution of the early universe and the formation of neutron stars. For this we need to study and understand how is the transition from this matter to a deconfinement phase, mixed phase and its critical end point, as well as to understand phenomena such as the restoration of chiral symmetry, among others.

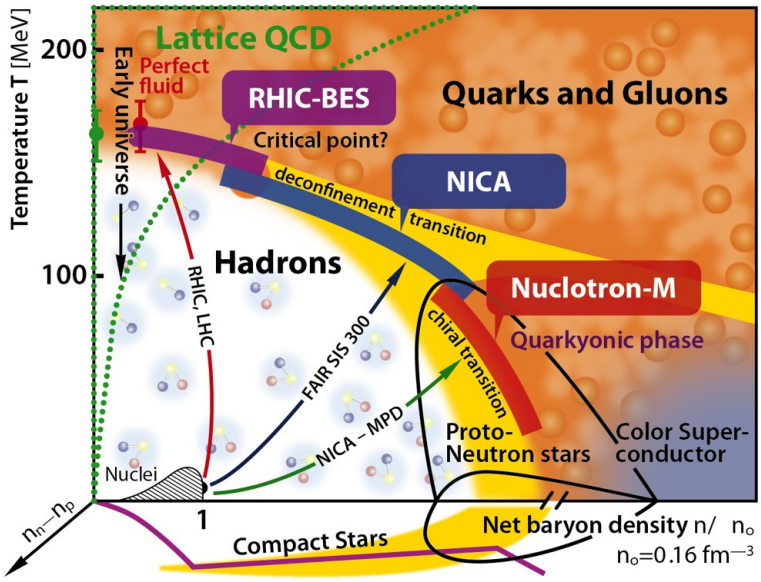

Figure 1.1: Phase diagram for nuclear matter [1].

In heavy-ion collisions, it is suggested that exists an non zero total angular momentum that affects the behavior of the QGP [2]. Figure 1.2 shows how the spectators of the beam and the target move in opposite directions with a speed close to the speed of light, the z component of the collective velocity in the system near the spectators is expected to be different from the collective velocity at the center of the collision [3].

The production of this orbital angular momentum can manifest as vorticity. In the heavy-ion physics community experimental and theoretical efforts have led to the extraction of the vorticity through measurements of spin polarization of Λ and $\bar{\Lambda}$ in Au+Au collisions [4–6].

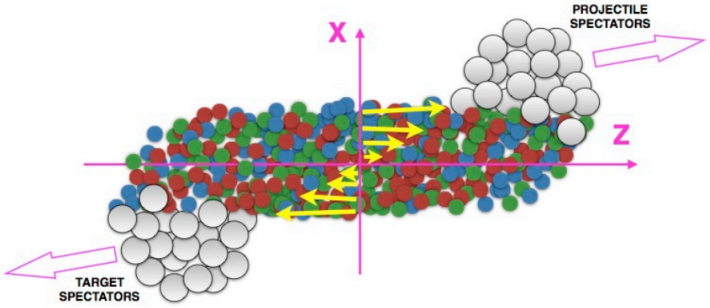

Figure 1.2: Sketch of a peripheral heavy ion collision. Arrows indicate the velocity flux [7].

1.2 Nucleotron-based Ion fAcility complex (NICA)

The Nucleotron-based Ion Collider fAcility (NICA) is the new accelerator of particles designed at Joint Institute of Nuclear Research (JINR). Its efforts are aimed to the study of nuclear matter in the regions of maximum baryonic density, as it should existed only at the early stages of the evolution of our Universe and in the interiors of neutron stars [8].

In figure 1.3, it is shown a sketch of the main elements of the NICA complex.There are an injection complex, which includes a set of ion sources and two linear accelerators, the super-conducting acting Booster, the superconducting acting synchrotron Nuclotron, a Collider composed of two superconducting rings with two beam interaction points, a Multi-Purpose Detector (MPD) and a Spin Physics Detector (SPD) and beam transport channels [9].

The NICA accelerator will provide variety of beam species ranged from protons and polarized deuterons to very massive gold ions. Heavy ions will be accelerated up to kinetic energy of 4.5 GeV per nucleon, the protons – up to 12.6 GeV.

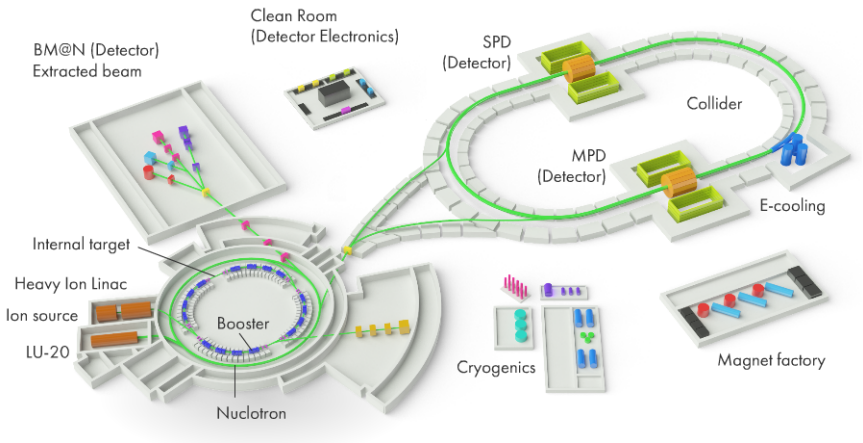

Figure 1.3: A diagram of NICA complex[8].

1.3 Multi-Purpose Detector (MPD)

The MPD has been designed as an spectrometer able to detect charged hadrons, electrons an photons, in the operating energy ranges of NICA. The detector will comprise a precise 3-D tracking system and a high-performance particle identification (PID) system based on the time-of-flight measurements and calorimetry.

At the design luminosity, the event rate in the MPD interaction region is about 6 kHz; the total charged particle multiplicity exceeds 1000 in the most central Au+Au collisions at $\sqrt{s_{NN}}$=11 GeV . As the average transverse momentum of the particles produced in a collision at NICA energies is below 500 MeV/c, the detector design requires a very low material budget [10].

Simulation done for Au+Au and B+Bi at NICA energies have shown that MPD experiment will be able to provide a good resolution of the event plane for measurements of direct and elliptic flows, and polarization. [11–13].

The aim of this Project is to build a first stage of the MPD setup, as shown in figure 1.4, which consists of the superconducting solenoid, Time-Projection Chamber (TPC), barrel Time-Of-Flight system (TOF), Electromagnetic Calorimeter (ECal), hadron calorimeter (FHCal) and Fast Forward Detector (FFD) 1.4.

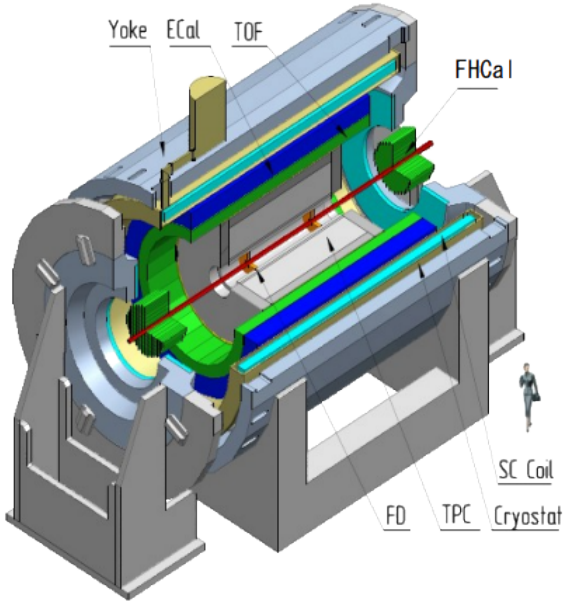

Figure 1.4: A general view of the MPD detector with end doors retracted for access to the inner detector components [14].

Chapter 2

Theoretical framework

2.1 Core Corona approach

In peripheral heavy-ion collisions, two regions can be identified as a high-density core and a less dense corona. If the total number of Λ coming from the core is N^{Λ}_{QGP} and N^{Λ}_{REC} is the number of Λ coming from the corona, the Core-Corona model allows to express the global polarization as

$$\mathcal{P}^{\Lambda} = \frac{\mathcal{P}^{\Lambda}_{REC} + z\frac{N_{\Lambda\ QGP}}{N_{\Lambda\ REC}}}{(1+\frac{N_{\Lambda\ QGP}}{N_{\Lambda\ REC}})}$$
$$\mathcal{P}^{\bar{\Lambda}} = \frac{\mathcal{P}^{\bar{\Lambda}}_{REC} + \bar{z}(\frac{w'}{w})\frac{N_{\Lambda\ QGP}}{N_{\Lambda\ REC}}}{(1+(\frac{w'}{w})\frac{N_{\Lambda\ QGP}}{N_{\Lambda\ REC}})} \tag{2.1}$$

Where $w' = \frac{N_{\bar{\Lambda}\ QGP}}{N_{\Lambda\ QGP}}$ and $w = \frac{N_{\bar{\Lambda}\ REC}}{N_{\Lambda\ REC}}$ are the ratio of the number of Λ and $\bar{\Lambda}$ in the core and in the corona respectively. z and$\bar{z}$ are intrinsic polarizations for Λ and $\bar{\Lambda}$. The quantities $\mathcal{P}^{\Lambda/\bar{\Lambda}}_{REC}$ are the contribution to global polarization from the Λ and $\bar{\Lambda}$ from the corona.

This model does a good average description of the global polarization obtained in semi-central collisions of heavy systems [15, 16], as a function of the collision energy, taking $\mathcal{P}^{\Lambda/\bar{\Lambda}}_{REC}$=0. However, these contributions become relevant of systems such as Ag+Ag at $\sqrt{s_{NN}}$=2.55 GeV, in the 10-40% centrality class, or Au+Au at $\sqrt{s_{NN}}$=3 GeV, for centralities larger than 40% [17].

Figure 2.1 shows an estimation of global polarization for $\sqrt{s_{NN}}$= 3 GeV. In the left panel, the contribution of polarization due the corona region is neglected. In the other hand, in the right panel it is considered a contribution from the corona of $\mathcal{P}^{\Lambda}_{REC}$=4%. This consideration improves a little the agreement between the estimated calculation and the experimental data. This suggest that we can improve our estimations of the

global polarization with a better understanding of the behavior of the contribution to polarization coming from the corona region.

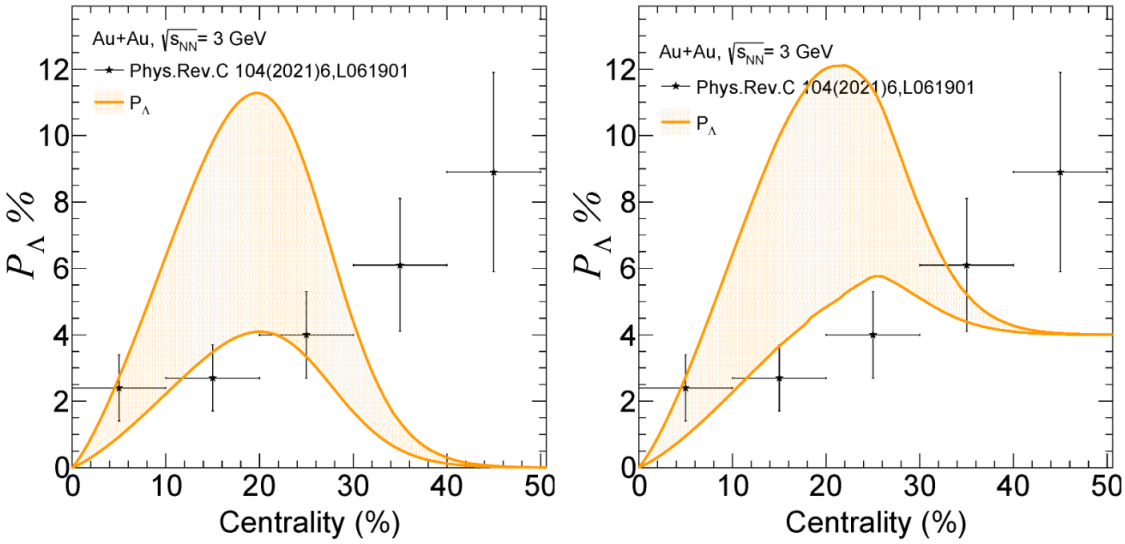

Figure 2.1: Λ global polarization as a function of centrality. With (right plot) and without (left plot) $\mathcal{P}^{\Lambda}_{REC}$=4% contribution for all centrality bins. Data for Au+Au at $\sqrt{s_{NN}}$=3 GeV [18].

2.2 Estimation of the polarization from the corona

In peripheral heavy-ion collisions, the core-corona model assumes that particles are produced by nucleon-nucleon interactions, due the critical density of participants to produce a QGP is barely or not achieved. Consequently, the polarization of Λ hyperons is produced during the hadronization process by an as yet unknown mechanism.

In p+p collisions, Λ transverse polarization $\mathcal{P}_\Lambda$ is different from zero [19–22]. So, we assume that the Λ produced in the corona shows a similar transverse polarization with respect to its production plane, then we project this polarization along the global polarization direction and estimate whether its contribution is different from zero.

This estimation can be done considering that each Λ is produced in a p+p collision from the participants in the corona and that its polarization points along the direction of the production plane $\hat{n}$, which is defined by the direction of the incoming proton $\vec{p}_{beam}$ and the Λ direction, $\vec{p}_\Lambda$. Taking the beam direction parallel to $\hat{z}$,

$$\hat{n} = \frac{\vec{p}_{beam} \times \vec{p}_\Lambda}{|\vec{p}_{beam} \times \vec{p}_\Lambda|} = \frac{1}{p_{T_\Lambda}}(-p_{y\Lambda}, p_{x\Lambda}, 0) \tag{2.2}$$

For simplicity, we consider that the polarization $\mathcal{P}_{REC}$ is only different from zero along $\hat{n}$. Therefore, its contribution to the global polarization can be determined using the angular distribution of protons produced in the weak of Λ, which are used to experimentally measure the polarization. This distribution is given by

$$\frac{dN}{d\Omega} = \frac{N}{4\pi}(1 + \alpha\mathcal{P}_{REC}\cos\sigma^*) \tag{2.3}$$

where α=0.732 [23] is the decay asymmetry parameter and σ^* is the angle between $\hat{n}$ and total angular momentum direction $\hat{L} = \hat{b} \times \hat{p}_{beam} = (\sin\Psi_{RP}, -\cos\Psi_{RP,0})$. Therefore,

$$\cos\sigma^* = \hat{n}\cdot\hat{L} = \frac{1}{p_{T_\Lambda}}(-p_{y\Lambda}\sin\Psi_{RP} + p_{x\Lambda}\cos\Psi_{RP}) \tag{2.4}$$

Now, we substitute

$$\begin{aligned} p_{x\Lambda} &= P_\Lambda \sin\theta_\Lambda \cos\phi_\Lambda \\ p_{y\Lambda} &= P_\Lambda \sin\theta_\Lambda \sin\phi_\Lambda \\ p_{T_\Lambda} &= P_\Lambda \sin\theta_\Lambda \end{aligned} \tag{2.5}$$

and we obtain

$$\cos\sigma^* = -\sin\phi_\Lambda \sin\Psi_{RP} - \cos\phi_\Lambda\cos\Psi_{RP} = -\cos(\phi_\Lambda - \Psi_{RP}) \tag{2.6}$$

Then, we can replace this last expression in Eq. (2.3) and integrate over the polar angle θ and obtain an expression for $\mathcal{P}_{REC}$ as

$$\mathcal{P}_{REC} = \frac{-2\langle\cos(\phi_\Lambda - \Psi_{RP})\rangle}{\alpha} \tag{2.7}$$

Then, we have two different methods to estimate corona polarization. We will call Eq. (2.3) the projection method and Eq. (2.7) the flow method. It is important to notice that the right-hand side of Eq. (2.7) appears also in the expression to determine the directed flow. Therefore, if the directed flow is non-vanishing, one can expect that the contribution to global Λ polarization in the corona is also non-vanishing [24].

2.3 Event shape variables

The event shape variables have been used in high energy physics to characterize events with jet structure. One of the most analyzed event shape variables the transverse sphericity ($S_\perp$). In [25, 26], $S_\perp$ has been employed to understand the dynamics of particle production mechanism in *pp* collisions at LHC energies. Monte Carlo simulations have also shown that different observables, like transverse momentum or multiplicity, are sensitive to $S_\perp$ and suggest that $S_\perp$ can be used to separate isotropic events from jetty-like events in *pp* collisions [27–30]. Also, another interesting, and relevant result for this project, is shown in [31]. In this work it is shown that the elliptic flow parameter for the jetty events are found to be much higher in magnitude than those obtained from both the

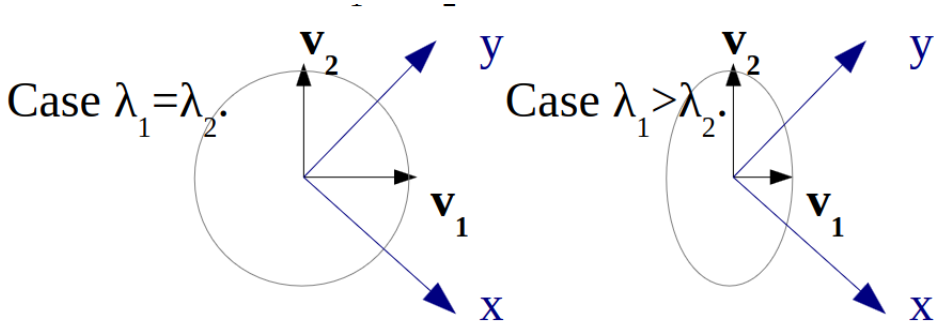

Figure 2.2: Sketch of two events with different transverse sphericity $S_\perp$. When $\lambda_1 = \lambda_2$, $S_\perp = 1$ and the event is isotropic. When $\lambda_1 >> \lambda_2$, $S_\perp \to 0$ and the event is jetty [33].

isotropic and entire class of events.

To define transverse sphericity we start from the transverse momentum matrix as

$$S_{xy} = \frac{1}{\sum_i p_{\perp i}} \frac{1}{\sum_i p_{\perp i}} \begin{pmatrix} p_{xi}^2 & p_{xi}\, p_{yi} \\ p_{yi}\, p_{xi} & p_{yi}^2. \end{pmatrix} \tag{2.8}$$

Here $p_{\perp i}$ is the transverse momentum of the ith particle in an event, and p_{xi} and p_{yi} are the components of $p_{\perp i}$. The sum runs over the particle number belonging to an event. The diagonalization of S_{xy} will lead to two eigenvalues, let us call them λ_1 and λ_2. We can assume that $\lambda_1 > \lambda_2$ to define the transverse sphericity as

$$S_\perp = \frac{2\lambda 2}{\lambda_1 + \lambda_2}. \tag{2.9}$$

The values of $S_\perp$ lies in the interval [0,1], the limit $S_\perp \to 0$ corresponds to jetty-like events, by the other hand the limit $S_\perp \to 1$ corresponds to isotropic events. [32]

Chapter 3

Methodology

3.1 General methodology

The main purpose of this work is estimate the Λ polarization in the corona region. In order to achieve this goal, we need to do several previous analysis to the data. These analysis will provide us all the information we need to make an estimation of polarization.

First, we need to separate events by centrality class. This will allow us to comprehend the behavior of polarization as function of centrality class, which is the usual way that polarization is reported.

Second, we need also to distinguish isotropic events from jetty events. As we discuss before, Eq. (2.7) relates corona polarization with directed flow, and the elliptic flow behaves different from events with low and high sphericity, that is an event shape variable capable to characterize jetty and isotropic events (see figure 2.2).

Once we have the events separated by centrality class and sphericity, we can estimate polarization using Eq. (2.3) or Eq. (2.7). But it is necessary to identify protons who decay from a Λ. Identify such protons is not a complex task by means of their PID, but this method of identification are not appropriate for real data. In this case, we need to reconstruct the Λ particle matching all protons and pions and estimate if a particular pair can be a Λ decay.

All these steps require a lot of work by their own, but the MPD collaboration group has several tools that helps and support the MPD experiment, the software framework MpdRoot that is being developed. It provides a powerful tool for detector performance studies, event simulation, and development of algorithms for reconstruction and physics analysis of data of the events registered by the MPD experiment.

3.2 MPDroot framework and analysis trains

For this project, we will analyse the following official NICA Monte Carlo data sets [34]:

- Request 30: General-purpose, PHSD Bi+Bi $\sqrt{s_{NN}}$=9.2 GeV.
- Request 25: General-purpose, UrQMD Bi+Bi $\sqrt{s_{NN}}$=9.2 GeV.

These data set are integrated in the MPDroot framework, the main computational tool of the MPD group [32]. The MPDroot framework is based on object oriented set of tools to simulate, transport and reconstruct MC events within MPD experiment. It provides a powerful tool for detector performance studies, event simulation, and development of algorithms for reconstruction and physics analysis of data of the events registered by the MPD experiment.

For analysis of big Monte Carlo data sets, was proposed to move to a centralized Analysis Framework. In this framework, analyses are grouped in a train, see figure 3.1, analyses are run simultaneously with a single access to data for all of them, reducing the number of input/output operations for disks and databases, easier organization of data storage.

Figure 3.1: Sketch of the train analysis. Analysis manager reads event into memory and calls wagons one-by-one to modify and/or analyze data [35].

3.2.1 Core-Corona analysis train

The analysis of the polarization with the core-corona model will be carried on in the Analysis Framework. With this goal, we need to call the necessary analysis wagons already availables. The core-corona analysis train is formed as follows

1. Centrality wagon → Analyses events and separate them by centrality class
2. Event plane wagon → Analyses events to obtain the angle between the momentum the particles of each event and the normal vector to the event plane.
3. evPID wagon → Identifies particles due their energy loss by means of their track in the TPC.

Centrality class	Jetty	Isotropic
0-10%	(0,0.8375)	(0.9275,1)
10-20%	(0,0.8275)	(0.9225,1)
20-30%	(0,0.8175)	(0.9125,1)
30-40%	(0,0.8025)	(0.9075,1)
40-50%	(0,0.7825)	(0.9025,1)
50-60%	(0,0.7625)	(0.8925,1)
60-70%	(0,0.7325)	(0.8775,1)
70-80%	(0,0.6925)	(0.8575,1)
80-90%	(0,0.6325)	(0.8275,1)
90-100%	(0,0.5275)	(0.7675,1)

Table 3.1: Limiting values of transverse sphericity for jetty and isotropic events for Req. 25 data (UrQMD).

4. Event Shape Analysis wagon → Analyse different event shape variables of each event.

The output file of the core-corona train is a root file with all the histograms necessary to make an estimation of the global polarization by centrality class, from Monte Carlo or from reconstructed data. Also, the Event Shape Analysis wagon allow us to separate isotropic and jetty events due to the sphericity of events.

3.3 Isotropic and jetty events

We will separate events in isotropic and jetty events according their sphericity. To do this, we will take the following procedure:

1. At a given centrality class, we will take N as all the events.
2. We will sum the events in each sphericity bin, starting from 0, the lowest value.
3. When the number of summed events N_{jet} is the 30% of N, we will stop.
4. We will consider N_{jet} as jetty events.
5. Doing steps 1-4 but starting from 1, the highest value, the N_{iso} value equal to 30% of N will be taken as isotropic events.

This procedure will provide us with sphericity intervals where the jetty and isotropic events are for each centrality class. Such intervals are enlisted in tables 3.1 for the UrQMD Req. 25 and 3.2 for the PHSD Req. 30.

Centrality class	Jetty	Isotropic
0-10%	(0,0.8775)	(0.9425,1)
10-20%	(0,0.8675)	(0.9375,1)
20-30%	(0,0.8575)	(0.9275,1)
30-40%	(0,0.8425)	(0.9225,1)
40-50%	(0,0.8325)	(0.9175,1)
50-60%	(0,0.8175)	(0.9075,1)
60-70%	(0,0.7975)	(0.8925,1)
70-80%	(0,0.7675)	(0.8775,1)

Table 3.2: Limiting values of transverse sphericity for jetty and isotropic events for Req. 30 data (PHSD).

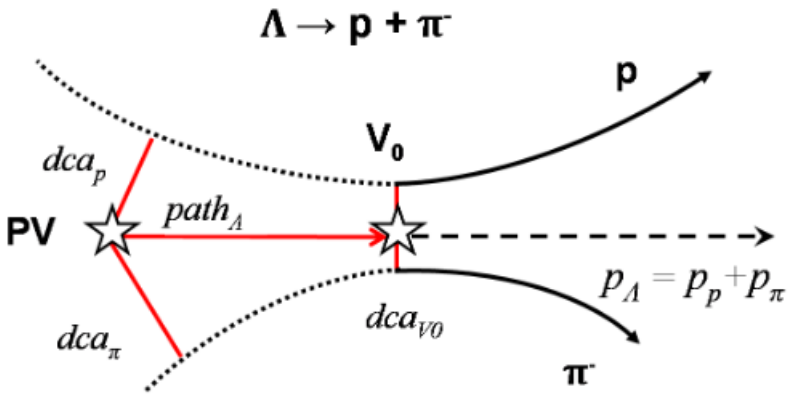

Figure 3.2: Topology of a Λ decay.

3.4 Reconstruction of Λ

The last considerations we need to take in account are cuts in some topological variables that will ensure that a proton-pion pair come from a Λ decay.

In Figure 3.2 is shown a sketch of the topology of a Λ decay. In this picture, **PV** represents the primary vertex, is the point in space at which the collision occurs. Particles coming from **PV** are called *primary particles*.

Neutral primary particles, as the Λ, cannot be detected directly, but by their decay products. The particles that comes from the decay of other particles are called *secondary particles*, and the point in space at the primary particle decays is called *secondary vertex*.

If we have two tracks identified as p and π^-, we need that the closest distance between them, called $\mathbf{dca_{V0}}$, be small. This will ensure that the pair $p\pi^-$ come from the same secondary vertex. The distances $\mathbf{dca_p}$ and $\mathbf{dca}_\pi$ are the closest distance between

p track and π^- track to **PV**. If these distance are small, the pair $p\pi^-$ comes from the **PV** and are primary partciles. So, to ensure that the pair are secondary particles, $\mathbf{dca_p}$ and $\mathbf{dca}_\pi$ should be large enough.

When a Λ is emitted from **PV**, travels a distance $\mathbf{path_\Lambda}$ and decays at $\mathbf{V_0}$. If $\mathbf{path_\Lambda}$ is short, the secondary vertex is at the same point that the **PV**. So, $\mathbf{path_\Lambda}$ should be large enough.

Another useful variable is the angle between $\mathbf{path_\Lambda}$ and $p_\Lambda = p_p + p_\pi$ vector. These two vectors should be parallel, so we expect that this angle is small, or the cosine of the angle close to 1.

In this work, we use the cuts in the variables showed in table 3.3, the χ^2 are calculated for the track with respect the primary vertex.

Variable	Cut
χ^2_{V0}	<7.0
angle	< 0.008
χ^2_p	> 5.0
χ^2_π	> 8.0
Invariant mass	$1.08 < m < 1.2$ GeV

Table 3.3: Cuts in the topological variables for Λ reconstruction.

Chapter 4

Results

4.1 Polarization of Monte Carlo data

The following result were obtained using Req. 30 data set, using 7M events. We estimate polarization using the projection method described in Eq. (2.3). We show in 4.1 the distribution of protons with respect the projection of the momentum with the normal of the reaction plane for jetty events in different centrality classes. We fit the data with the Eq. (2.3), and the parameter P is our estimation of the local polarization. For isotropic events, the procedure is similar and the results are shown in figure 4.2. We compare the behavior of local polarization as function of centrality class for jetty and isotropic events in figure 4.5.

For global polarization we followed a similar procedure. In 4.3, the distribution of protons with respect the projection of the momentum of the protons with event plane is shown for jetty events in different centrality classes. We fit the data with the Eq. (2.3), and the parameter P is our estimation of the global polarization. Of isotropic events, the procedure is similar and the results are shown in figure 4.4. We compare the behavior of global polarization as function of centrality class for jetty and isotropic events in figure 4.6.
Now, we analyse global polarization with the flow method described in Eq. (2.7). In figure 4.7, the distribution of protons with respect $\Delta\phi = \phi - \Psi_{rp}$ is shown for jetty events in different centrality classes. Our estimation of the global polarization is now $P = \frac{8b_1}{\alpha\pi}$. For isotropic events, the procedure is similar and the results are shown in figure 4.8. We compare the behavior of global polarization as function of centrality class for jetty and isotropic events in figure 4.9. We can compare figures 4.6 and 4.9 and notice that behavior of polarization for jetty and isotropic are similar in projection and flow method.

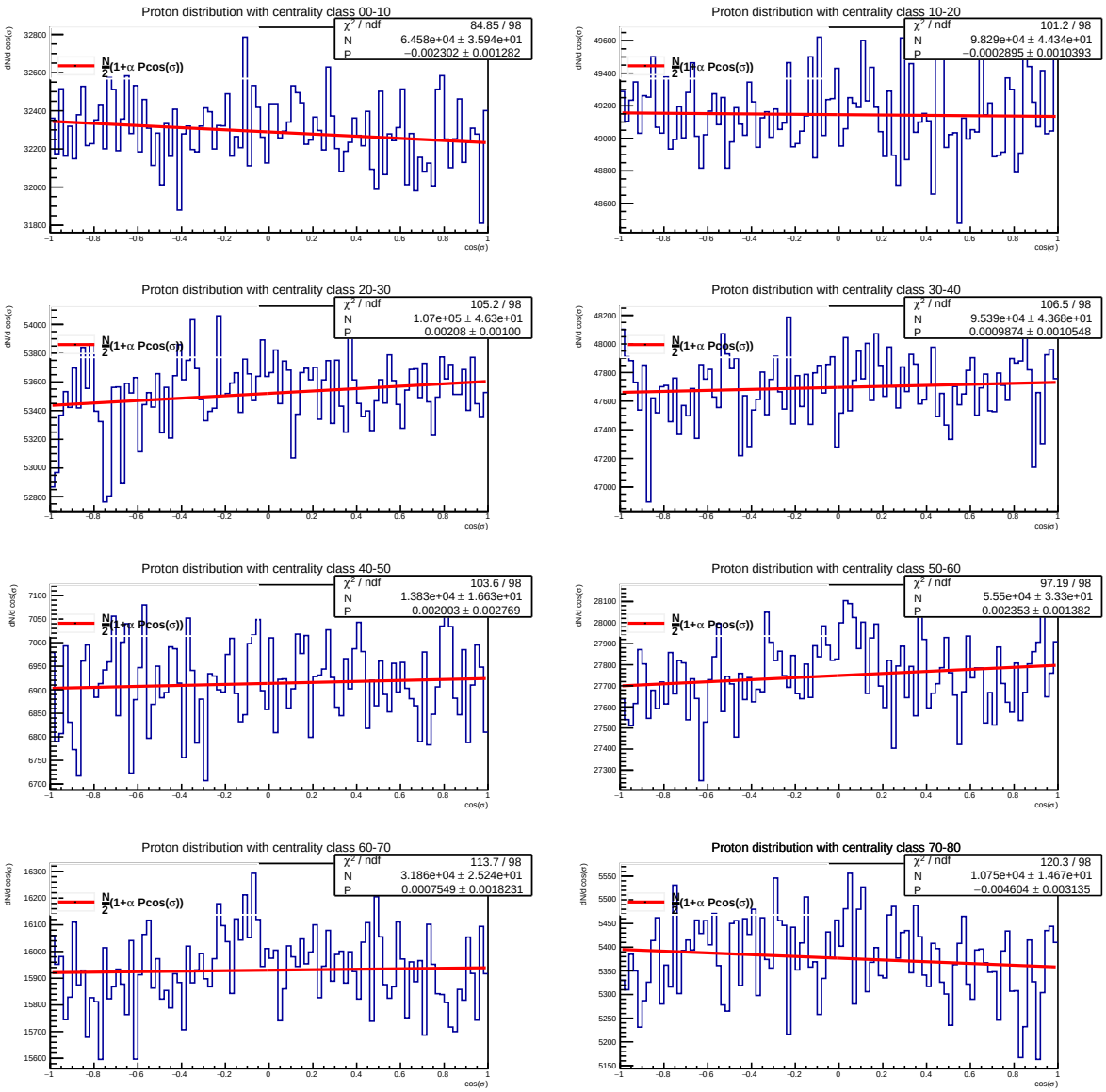

Figure 4.1: Distribution of protons with respect the angle between their momentum and the reaction plane for several centrality bins for jetty events. The parameter P in the fit estimates the local polarization. The data is obtained from Req. 30, using 7M events.

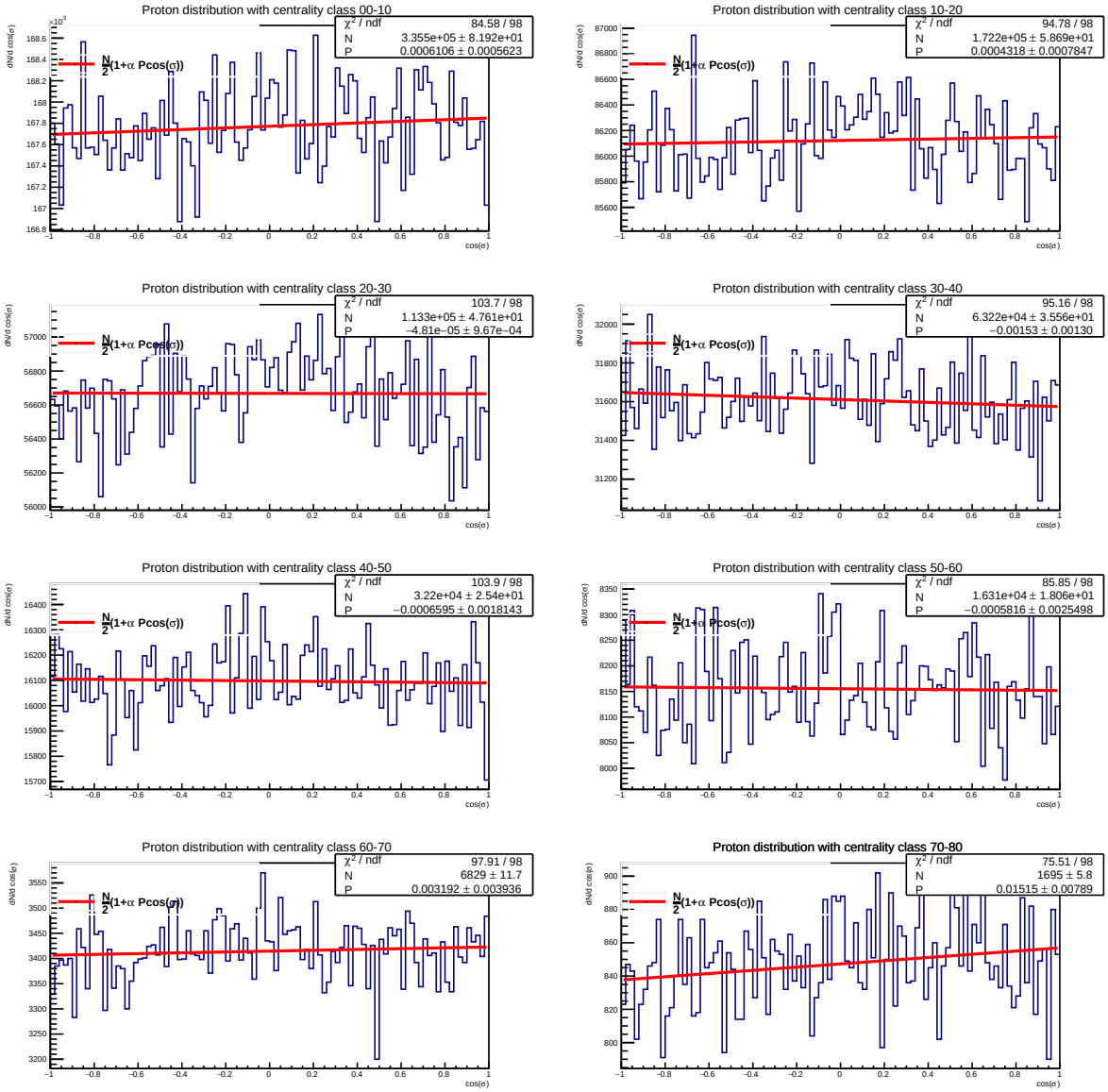

Figure 4.2: Distribution of protons with respect the angle between their momentum and the reaction plane for several centrality bins for isotropic events. The parameter P in the fit estimates the local polarization. The data is obtained from Req. 30, using 7M events.

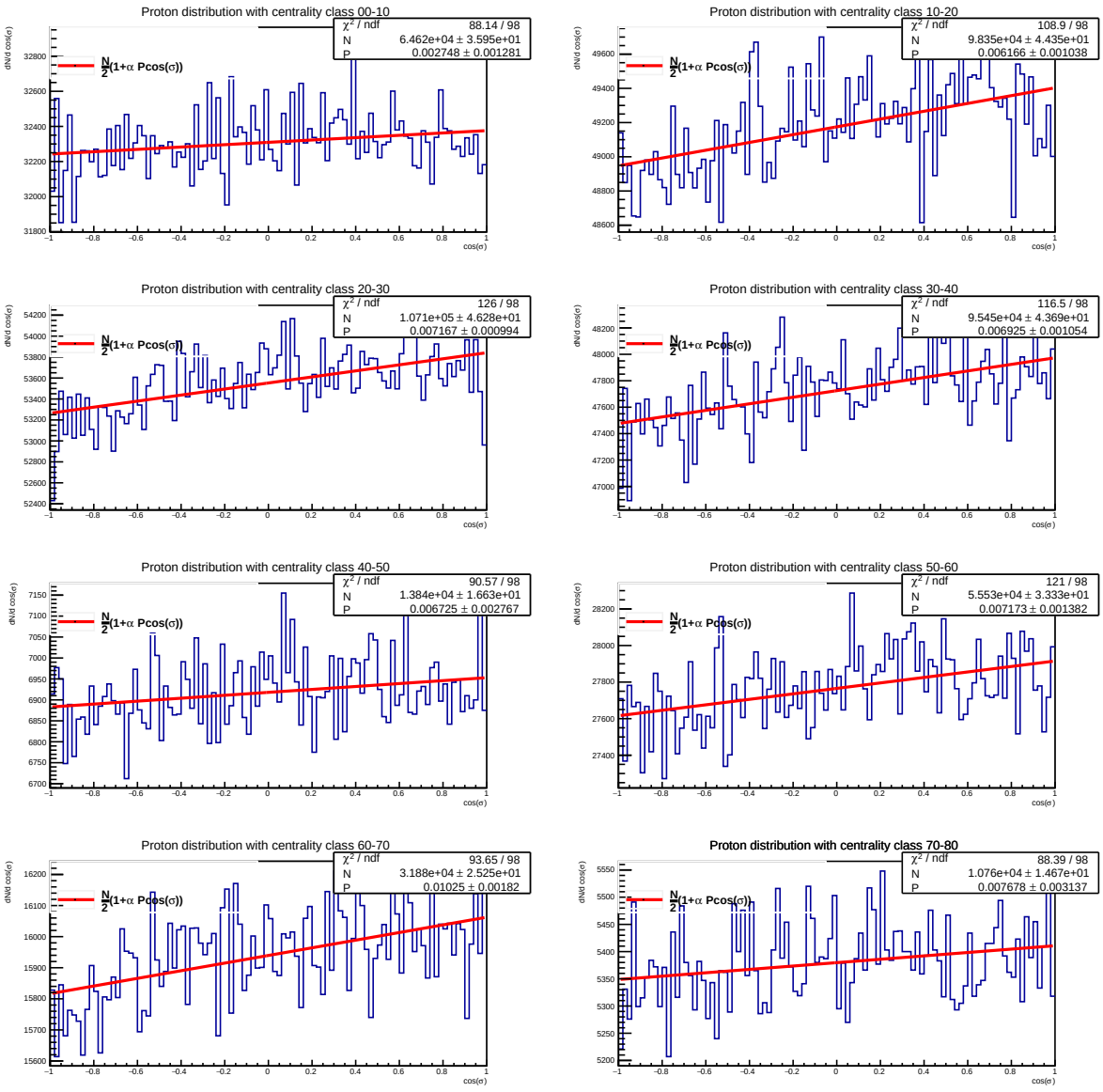

Figure 4.3: Distribution of protons with respect the angle between their momentum and the event plane for several centrality bins for jetty events. The parameter P in the fit estimates the local polarization. The data is obtained from Req. 30, using 7M events.

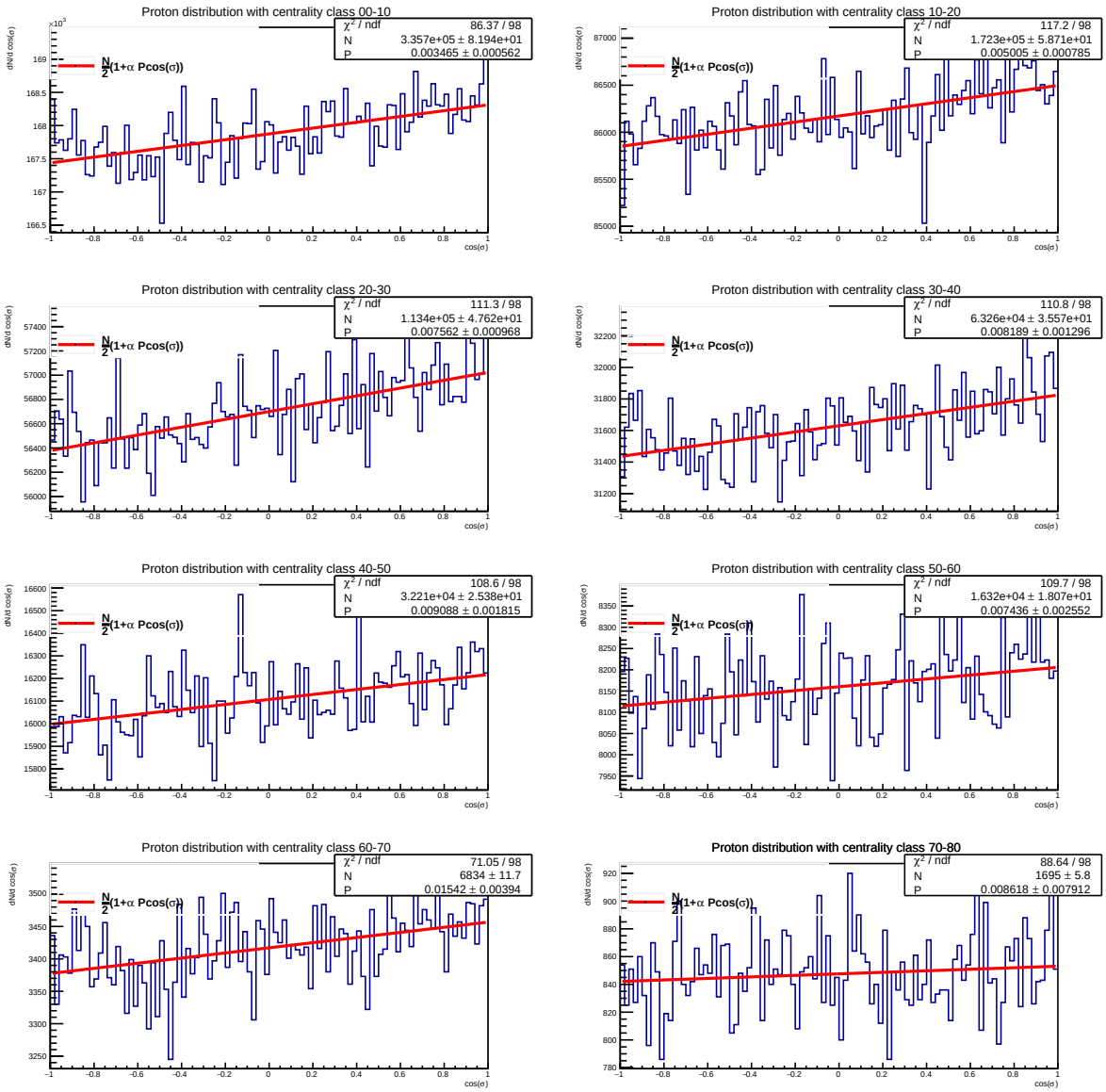

Figure 4.4: Distribution of protons with respect the angle between their momentum and the event plane for several centrality bins for isotropic events. The parameter P in the fit estimates the local polarization. The data is obtained from Req. 30, using 7M events.

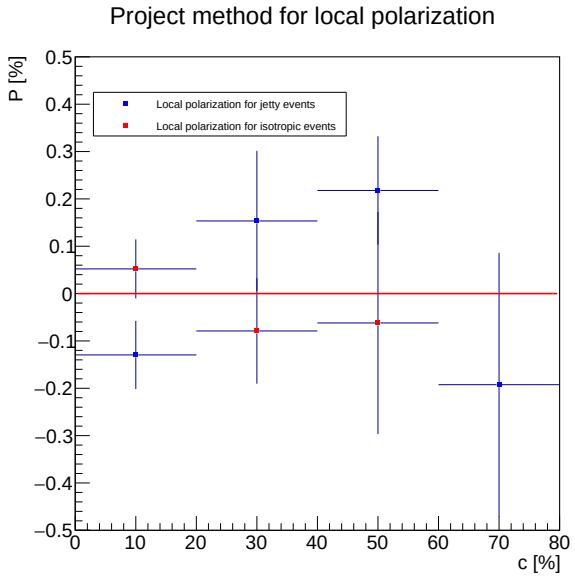

Figure 4.5: Local polarization as function of centrality class for jetty (blue) and isotropic (red) events.

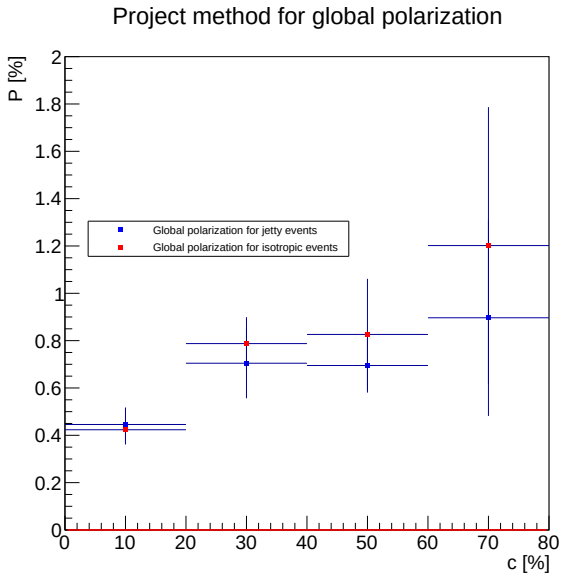

Figure 4.6: Global polarization as function of centrality class for jetty (blue) and isotropic (red) events.

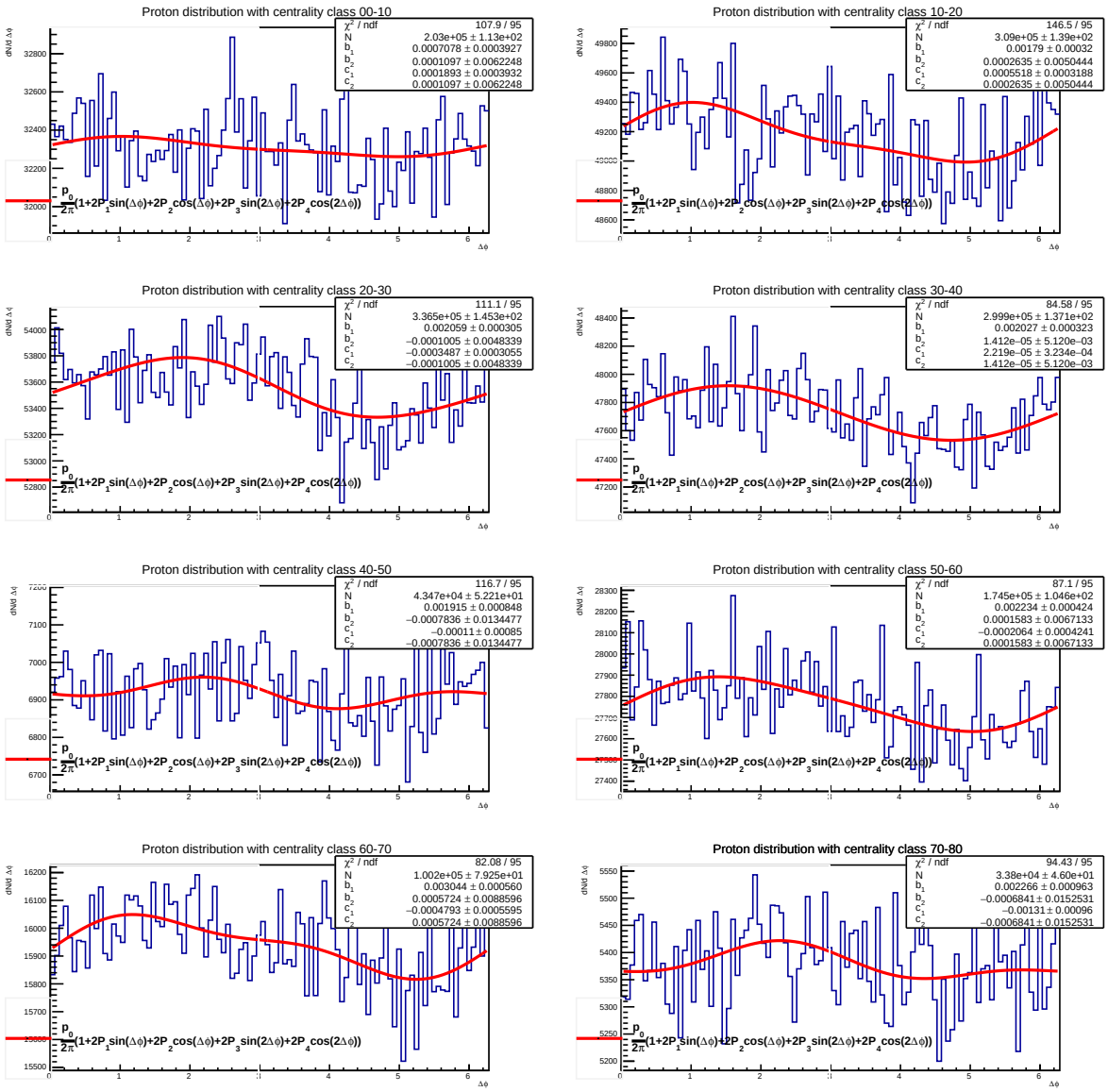

Figure 4.7: Distribution of protons with respect $\Delta\phi$ for several centrality bins for jetty events. The parameter P in the fit estimates the local polarization. The data is obtained from Req. 30, using 7M events.

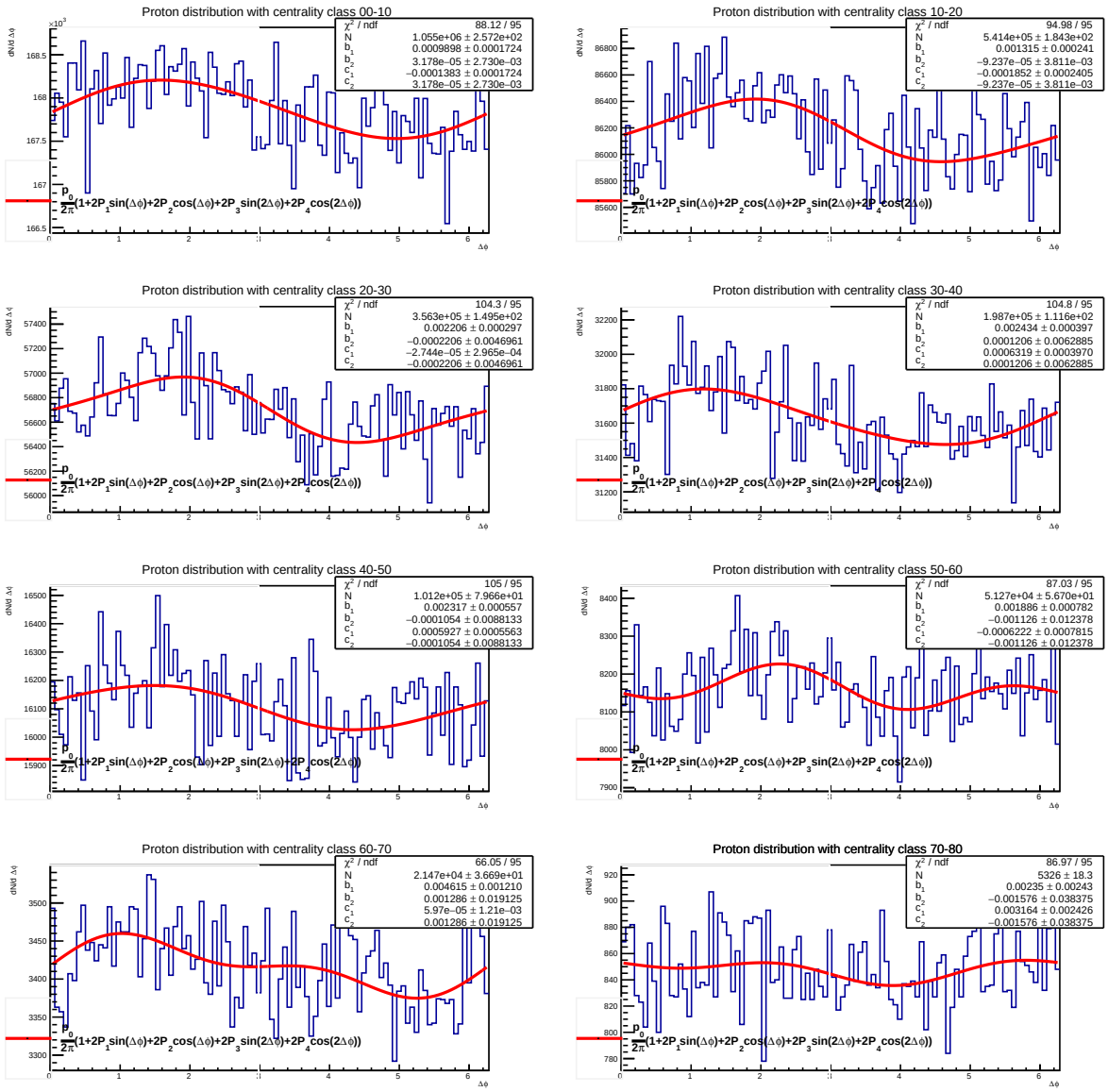

Figure 4.8: Distribution of protons with respect $\Delta\phi$ for several centrality bins for isotropic events. The parameter P in the fit estimates the local polarization. The data is obtained from Req. 30, using 7M events.

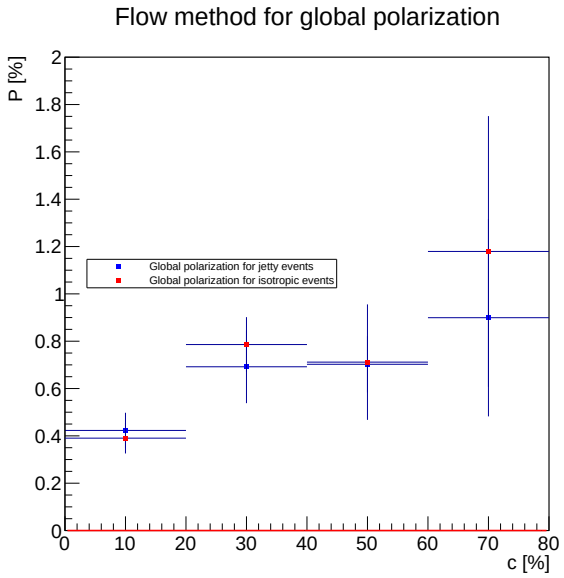

Figure 4.9: Local polarization as function of centrality class for jetty (blue) and isotropic (red) events.

4.2 Invariant mass for reconstructed Λ

The invariant mass obtained for our reconstruction of Λ is shown in figure 4.10 above. Also, the Armenteros-Podolaski plot for reconstructed Λ is shown in figure 4.10 below. Besides reconstructed Λ exhibits the expected behavior in invariant mass and Armenteros-Podolanski plot, reconstruction may be improved as future work.

4.3 Polarization of reconstructed and associated data

Once we have reconstructed data, we can analyse their polarization. In figure 4.11, the distribution of protons with respect $\Delta\phi = \phi - \Psi_{rp}$ is shown for reconstructed events in different centrality classes. Our estimation of the global polarization is now $P = \frac{8b_1}{\alpha\pi R^1_{EP}}$, with R^1_{EP} the resolution of the event plane. For associated events, the procedure is similar and the results are shown in figure 4.12. We compare the behavior of global polarization as function of centrality class for reconstructed and associated events in figure 4.13. The precision in this calculations is related with the quality of the reconstruction. Hence, it is a work in progress.

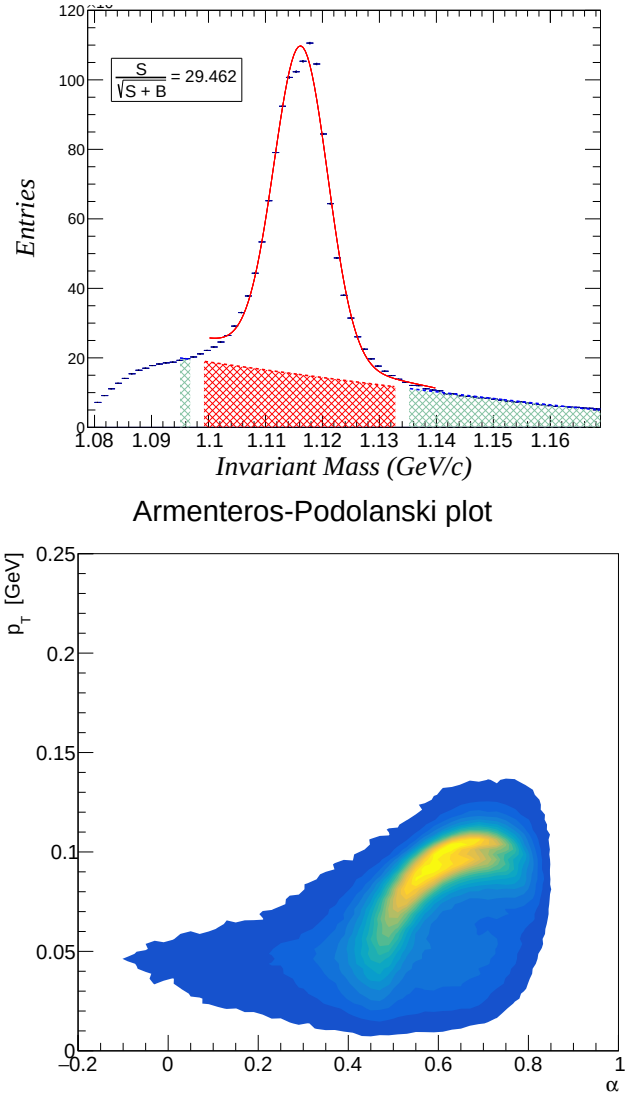

Figure 4.10: Above, the significance of the invariant mass signal. Below, the Armenteros-Podolanski plot for reconstructed Λ. Te reconstruction was made with the data obtained from Req. 30, using 7M events.

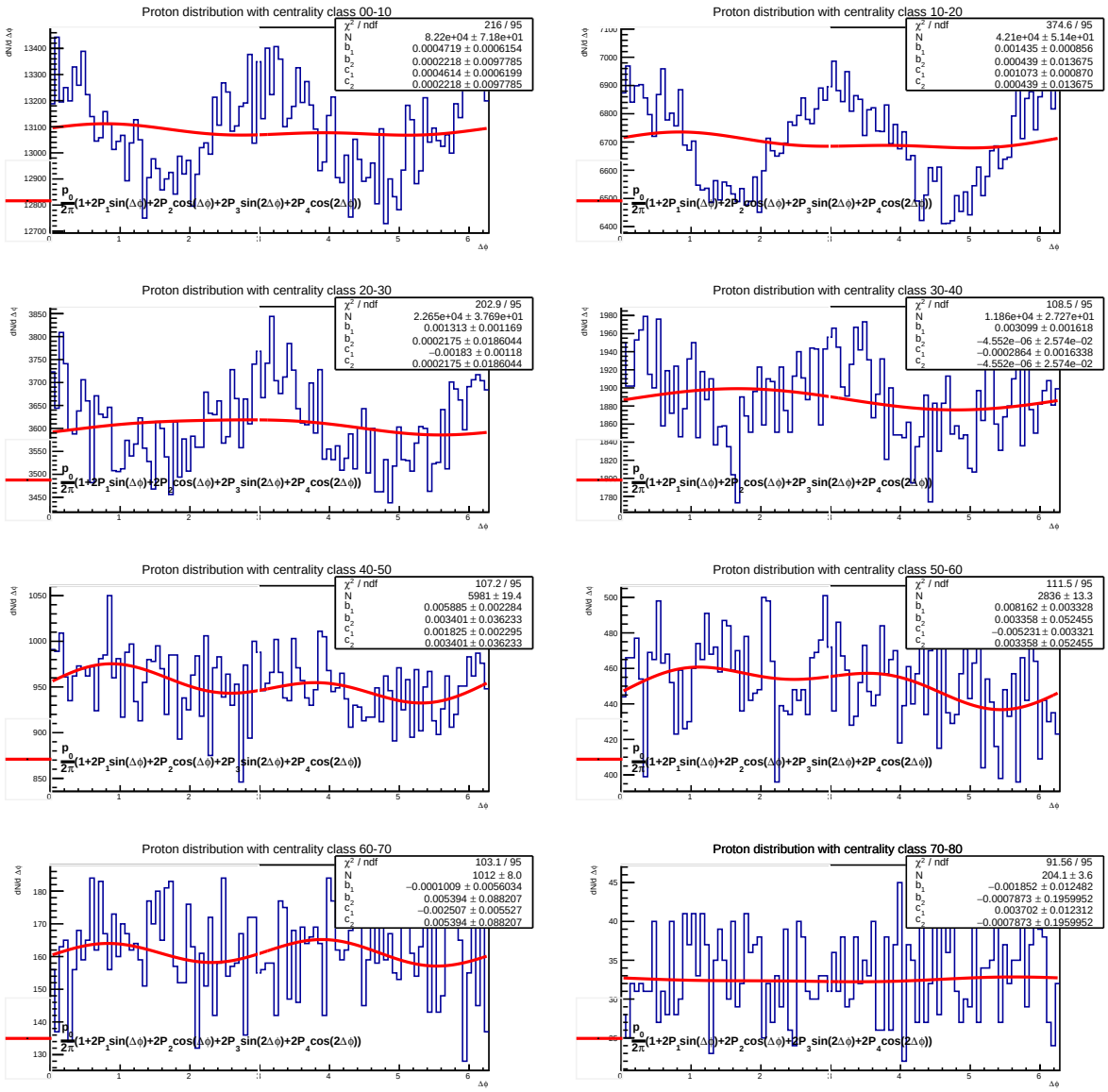

Figure 4.11: Distribution of protons with respect $\Delta\phi$ for several centrality bins for reconstructed events. The parameter P in the fit estimates the local polarization. The data is obtained from Req. 30, using 7M events.

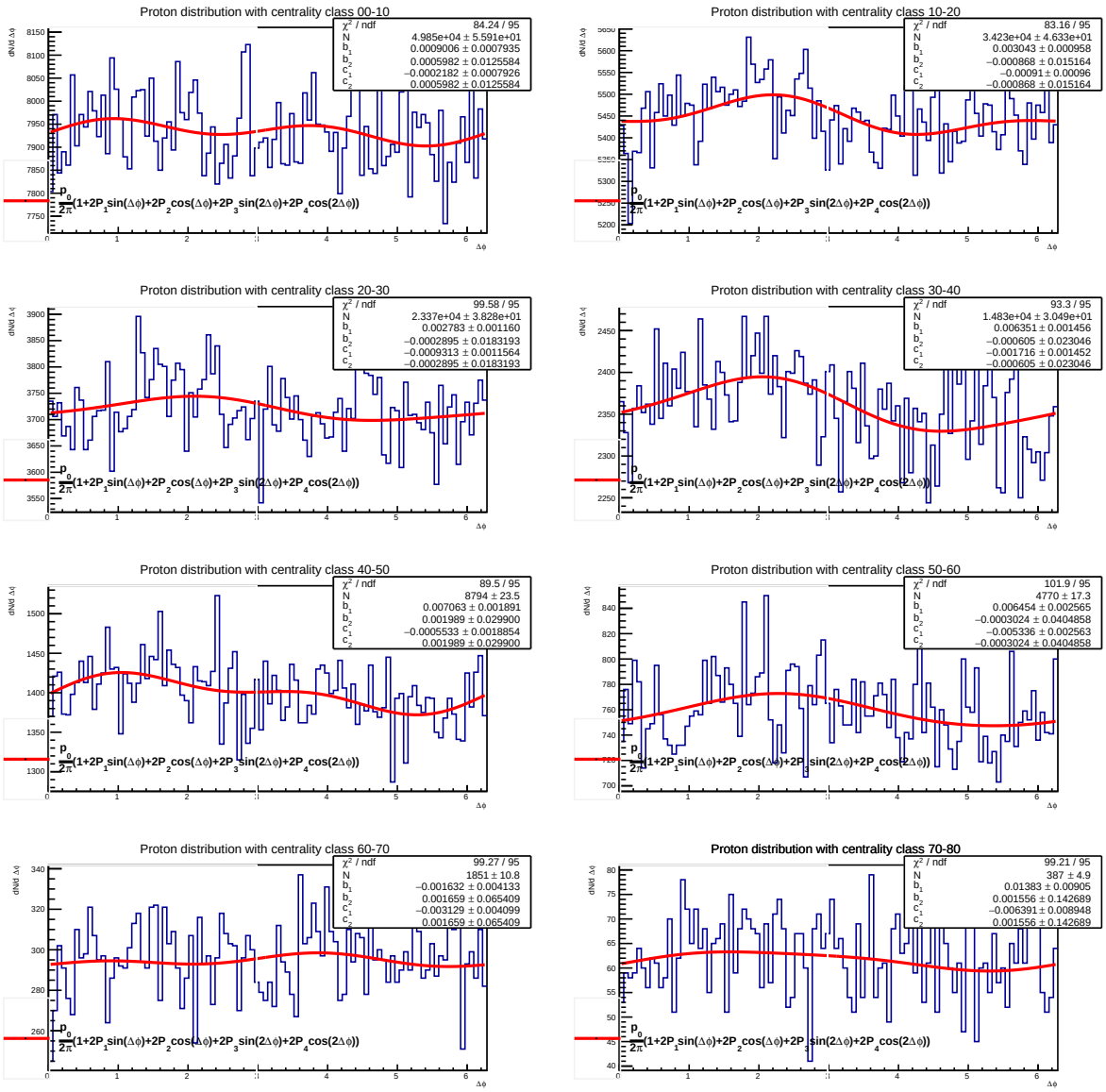

Figure 4.12: Distribution of protons with respect $\Delta\phi$ for several centrality bins for associated events. The parameter P in the fit estimates the local polarization. The data is obtained from Req. 30, using 7M events.

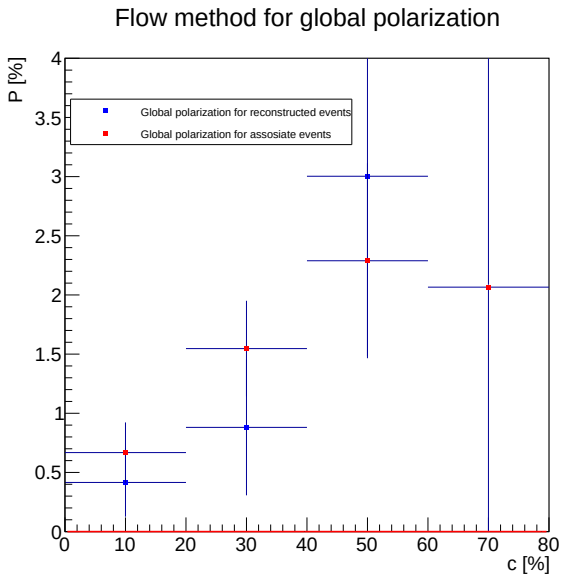

Figure 4.13: Local polarization as function of centrality class for reconstructed (blue) and associated (red) events.

Chapter 5

Conclusions

In this work, we estimate the local and global polarization of Λ hyperons for an energy Bi+Bi collisions at $\sqrt{s_{NN}}$=9.2 GeV using the Monte Carlo data set Req. 30. The most important feature of this work was the identification of jetty and isotropic events. We assume from previous works that jetty events have a sphericity value close to 0 and isotropic events a sphericity value close to 1. We calculate at which sphericity bin we have the 30% of the total events, from a lower limit and from an upper limit and we take these events as jetty and isotropic respectively for each centrality bin.

The separation of jetty and isotropic events allow us to study their polarization independently. From figure 4.5, we conclude that local polarization in both type of events is close to zero, which is expected for this PHSD data set. In the other hand, figure 4.6 shows that polarization is different from 0 for both cases. But also suggest that polarization of isotropic events are a little larger than for jetty events.

For reconstructed Λ, we identify secondary protons and pions using the evPID wagon and applied cuts in topological variables of the decay. Figure 4.10 shows the histogram of invariant mass and its analysis of significance y the upper part. Below, figure 4.10 shows the Armenteros-Podolanski plot, with the characteristic arch of Λ hyperons. Reconstruction can be improved optimizing the cuts. An analysis for polarization for these reconstructed events were carried out.

Besides the results achieved in this work, several important skills were developed. I learned how to work in the MPDroot framework or create and modify analysis trains in order to obtain certain result. Also, I learned a lot of technical and important features of the NICA experiment, that help us to focus our analysis. In the case of this work, the MPD characteristics are important to define the cuts on the topological variables and Λ reconstruction.

In summary, the principal goals achieved in this work were

- Familiarization with MPDroot framawork and another important tools for analysis

in the MPD collaboration.

- Implementation of Analysis Framework to the Core-Corona analysis.
- Obtaining an estimation of polarization in the framework.
- Identification of jetty and isotropic events due its sphericity.
- Analysis of the polarization for jetty and isotropic events.
- Reconstruction of Λ particle.
- Analysis of the polarization for reconstructed events.

Bibliography

[1] N. physics at JINR (official Web-Page), "NICA physics, url = https://nica.jinr.ru/physics.php,," .

[2] F. Becattini and M. Lisa, "Polarization and vorticity in the quark gluon plasma," arXiv preprint arXiv:2003.03640 (2020).

[3] X.-L. Xia, H. Li, Z. Tang, and Q. Wang, "Probing vorticity structure in heavy-ion collisions by local λ polarization," Physical Review C **98**, 024905 (2018).

[4] L. Adamczyk, J. Adkins, G. Agakishiev, M. Aggarwal, Z. Ahammed, N. Ajitanand, I. Alekseev, D. Anderson, R. Aoyama, A. Aparin, *et al.*, "Global λ hyperon polarization in nuclear collisions," Nature (London) **548** (2017).

[5] J. Adam, L. Adamczyk, J. Adams, J. K. Adkins, G. Agakishiev, M. Aggarwal, Z. Ahammed, N. Ajitanand, I. Alekseev, D. Anderson, *et al.*, "Global polarization of λ hyperons in au+ au collisions at s n n= 200 gev," Physical Review C **98**, 014910 (2018).

[6] J. Adam, L. Adamczyk, J. Adams, J. Adkins, G. Agakishiev, M. Aggarwal, Z. Ahammed, I. Alekseev, D. Anderson, R. Aoyama, *et al.*, "Polarization of λ (λ^-) hyperons along the beam direction in au+ au collisions at s n n= 200 gev," Physical review letters **123**, 132301 (2019).

[7] I. Karpenko, "Vorticity and polarization in heavy ion collisions: Hydrodynamic models," arXiv preprint arXiv:2101.04963 (2021).

[8] J. I. for Nuclear Research, "Nucleotron-based Ion Collider fAcility (NICA), url = https://nica.jinr.ru/,," .

[9] A. Butenko, S. Kostromin, I. Meshkov, A. Sidorin, E. Syresin, H. Khodzhibagiyan, and G. Trubnikov, "The nica complex injection facility," Proc. of RUPAC **21** (2021).

[10] V. Golovatyuk, V. Kekelidze, V. Kolesnikov, O. Rogachevsky, and A. Sorin, "The multi-purpose detector (mpd) of the collider experiment," The European Physical Journal A **52**, 1–7 (2016).

[11] A. Taranenko, "Status of the mega-science project nica," in *Journal of Physics: Conference Series*, Vol. 1685 (IOP Publishing, 2020) p. 012021.

[12] L. Malinina, P. Batyuk, M. Cheremnova, Y. Khyzhniak, O. Kodolova, K. Mikhaylov, G. Nigmatkulov, and G. Romanenko, "Study of strongly interacting matter properties at the energies of the nica collider using the methods of femtoscopy," Physics of Particles and Nuclei **52**, 624–630 (2021).

[13] A. Ayala, E. Cuautle, I. Domínguez, M. Rodríguez-Cahuantzi, I. Maldonado, and M. E. Tejeda-Yeomans, "Hyperons from bi+ bi collisions at mpd-nica: Preliminary analysis of production at generation, simulation and reconstruction level," Physics of Particles and Nuclei **52**, 730–736 (2021).

[14] K. U. Abraamyan, S. Afanasiev, V. Alfeev, N. Anfimov, D. Arkhipkin, P. Z. Aslanyan, V. Babkin, M. Baznat, S. Bazylev, D. Blaschke, *et al.*, "The mpd detector at the nica heavy-ion collider at jinr," Nuclear Instruments and Methods in Physics Research Section A: Accelerators, Spectrometers, Detectors and Associated Equipment **628**, 99–102 (2011).

[15] A. Ayala, M. A. A. Torres, E. Cuautle, I. Dominguez, M. A. F. Sanchez, I. Maldonado, E. Moreno-Barbosa, P. Nieto-Marín, M. Rodriguez-Cahuantzi, J. Salinas, *et al.*, "Core meets corona: A two-component source to explain λ and λ global polarization in semi-central heavy-ion collisions," Physics Letters B **810**, 135818 (2020).

[16] A. Ayala, I. Domínguez, I. Maldonado, and M. E. Tejeda-Yeomans, "Rise and fall of λ and λ^- global polarization in semi-central heavy-ion collisions at hades, nica and rhic energies from the core-corona model," Physical Review C **105**, 034907 (2022).

[17] A. Ayala, I. Domínguez, I. Maldonado, and M. E. Tejeda-Yeomans, "λ and $\bar{\Lambda}$ global polarization from the core-corona model," arXiv preprint arXiv:2207.10560 (2022).

[18] A. Ayala, I. Dominguez, I. Maldonado, and M. E. Tejeda-Yeomans, "An improved core-corona model for λ and λ polarization in relativistic heavy-ion collisions," Particles **6**, 405–415 (2023).

[19] A. Smith, R. Bonino, A. Castellina, S. Erhan, N. Medinnis, P. Schlein, P. Sherwood, S. Vernetto, J. Zweizig, J. Alitti, *et al.*, "λ0 polarization in proton-proton interactions from s= 31 to 62 gev," Physics Letters B **185**, 209–212 (1987).

[20] V. Blobel, H. Fesefeldt, W. Geist, U. Idschok, D. Lüers, B.-H.-M. M. Collaboration, *et al.*, "Transverse momentum dependence in proton-proton interactions at 24 gev/c," Nuclear Physics B **122**, 429–434 (1977).

[21] M. Asai, J. Marin, P. Porth, V. Stopchenko, C. Caso, M. Regler, P. Stamer, W. Bugg, J. Hrubec, A. Ferrando, *et al.*, "Inclusive k^0,λ and $\bar{\lambda}$ production in 360 gev/c pp interactions using the european hybrid spectrometer," Z. Phys. C **27**, 11–19 (1984).

[22] K. Jaeger, D. Colley, L. Hyman, and J. Rest, "Characteristics of v 0 and γ production in pp interactions at 205 gev/c," Physical Review D **11**, 2405 (1975).

[23] "Polarization and entanglement in baryon–antibaryon pair production in electron–positron annihilation," Nature Physics **15**, 631–634 (2019).

[24] A. Ayala, I. Domínguez, I. Maldonado, and M. E. Tejeda-Yeomans, "Core-corona approach to describe hyperon global polarization in semi-central relativistic heavy-ion collisions," arXiv preprint arXiv:2301.07356 (2023).

[25] B. Abelev, J. Adam, D. Adamová, A. Adare, M. Aggarwal, G. Aglieri Rinella, A. Agocs, A. Agostinelli, S. Aguilar Salazar, Z. Ahammed, *et al.*, "Transverse sphericity of primary charged particles in minimum bias proton-proton collisions at $\sqrt{s_{NN}}$ =0.9, 2.76 and 7 tev," The European Physical Journal C **72**, 1–16 (2012).

[26] A. C. atlas. publications@ cern. ch, G. Aad, B. Abbott, J. Abdallah, S. Abdel Khalek, A. Abdelalim, O. Abdinov, B. Abi, M. Abolins, O. AbouZeid, *et al.*, "Measurement of event shapes at large momentum transfer with the atlas detector in pp collisions at s=7\mathrmtev," The European Physical Journal C **72**, 1–22 (2012).

[27] A. Ayala, E. Cuautle, I. Domínguez, A. Ortiz, and G. Paić, "Fine structure in the azimuthal transverse momentum correlations at gev using the event shape analysis," The European Physical Journal C **62**, 535–540 (2009).

[28] E. Cuautle, A. Ortiz, and G. Paic, "Sensitivity of the parameters measured in pp collisions on the gluon pdf," arXiv preprint arXiv:1001.0613 (2010).

[29] E. Cuautle, I. Domínguez, and G. Paić, "Jets structure in pb-pb collisions at lhc energies," in *Journal of Physics: Conference Series*, Vol. 287 (IOP Publishing, 2011) p. 012032.

[30] M. Fernández, E. Cuautle, and G. Paić, "Event shape variables, a tool for qcd study," in *Journal of Physics: Conference Series*, Vol. 761 (IOP Publishing, 2016) p. 012031.

[31] S. Sarkar, P. Mali, and A. Mukhopadhyay, "Transverse sphericity based event classification in au+ au collision at e lab= 30 a gev in a multi phase transport model," The European Physical Journal A **58**, 139 (2022).

[32] M. (official Web-Page), "MPDroot framework," .

[33] A. Banfi, G. P. Salam, and G. Zanderighi, "Phenomenology of event shapes at hadron colliders," Journal of High Energy Physics **2010**, 1–66 (2010).

[34] M. forum (official Web-Page), "MPD forum," .

[35] V. Riabov, "Analysis Framework," .